RSC Advances

This is an *Accepted Manuscript*, which has been through the Royal Society of Chemistry peer review process and has been accepted for publication.

Accepted Manuscripts are published online shortly after acceptance, before technical editing, formatting and proof reading. Using this free service, authors can make their results available to the community, in citable form, before we publish the edited article. This *Accepted Manuscript* will be replaced by the edited, formatted and paginated article as soon as this is available.

You can find more information about *Accepted Manuscripts* in the Information for Authors.

Please note that technical editing may introduce minor changes to the text and/or graphics, which may alter content. The journal's standard Terms & Conditions and the Ethical guidelines still apply. In no event shall the Royal Society of Chemistry be held responsible for any errors or omissions in this *Accepted Manuscript* or any consequences arising from the use of any information it contains.

ROYAL SOCIETY OF CHEMISTRY

www.rsc.org/advances

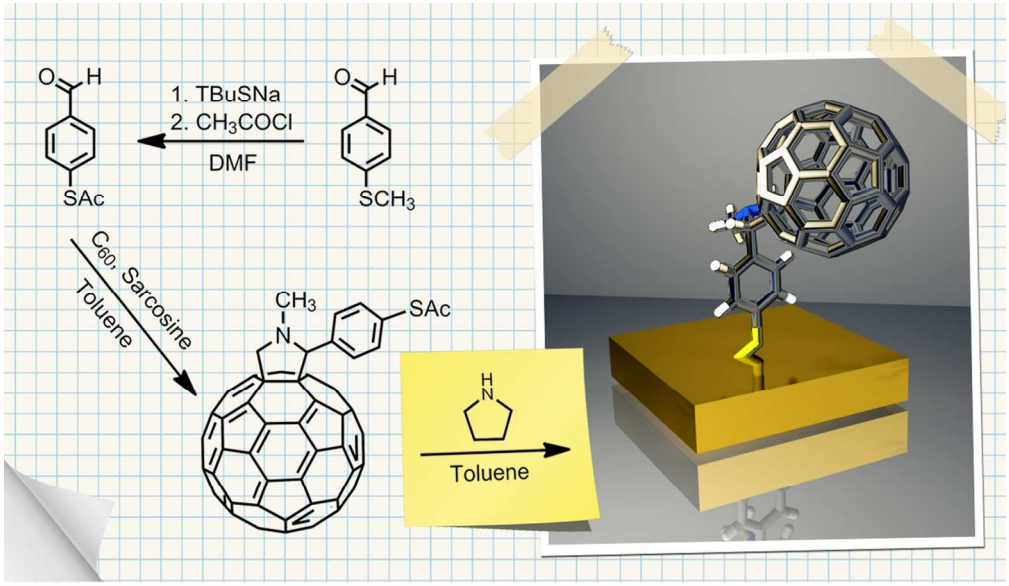

Two types of nanocomposites were synthesized: Au electrode covered with self-assembled *in situ* deprotected aromatic *S*-acetyl-derivatized C_{60} fullerenes and Au nanoparticles decorated with high number of C_{60} fullerenes.
111x64mm (300 x 300 DPI)

RSC Advances Accepted Manuscript

Journal Name

RSCPublishing

ARTICLE

Fullerene Modification of Gold Electrodes and Gold Nanoparticles Based on Application of Aromatic Thioacetate-Functionalized C_{60}

Cite this: DOI: 10.1039/x0xx00000x

Received 00th January 2012,
Accepted 00th January 2012

DOI: 10.1039/x0xx00000x

www.rsc.org/

Piotr Piotrowski[a], Joanna Pawłowska[a], Jan Pawłowski[b], Lidia Jagoda Opuchlik[a], Renata Bilewicz[a], Andrzej Kaim[a*]

A new procedure for the synthesis of S-acetyl-derivatized fullerene is described. The deprotected aromatic S-acetyl-derivatized fullerene was employed for efficient modification of gold electrode and gold nanoparticles. The proposed deposition procedure of fullerene derivative at Au surfaces allows the control of the thickness of the self-assembled fullerene layer. The modified surfaces were characterized by electrochemical methods and X-ray photoelectron spectroscopy (XPS). Functionalized fullerenes largely retain favorable redox electronic properties, behaving as an electron sink and revealing 4 reversible sequential 1e electrode processes at slightly more negative potentials than those observed for unsubstituted C_{60}. For the first time, fullerene-capped gold nanoparticles were obtained by a two - step ligand exchange procedure involving substitution of alkanethiol with thiolated fullerene derivative following the synthesis of alkanethiol capped nanoparticles. The ligand exchange procedure was very efficient – the number of fullerene moieties per single gold nanoparticle was found to be as high as 30.

Introduction

Fullerenes and their derivatives attract reasonable attention due to their unique electronic properties including reversible reduction with up to six electrons per single C_{60} molecule.[1] This gives them huge potential as building blocks for the construction of nanodevices[2] including well-ordered monolayers or thin films for practical applications in photovoltaic cells, field effect transistors, sensors, molecular wires or optoelectronics.[3,4]

The thiol moiety is the most widely used anchoring group for the modification of metals surfaces. Although the literature on thiol self-assembly on gold surface is very extensive and these structures have been thoroughly investigated, thiol functionalized fullerenes applications were limited to alkyl derivatives.[5] Due to the conductive and electronic properties, the aromatic thiols are more interesting for future implementations but reports on the subject are scarce[6] even though linker's structure and length may improve the electrical contact between the fullerene moiety and the gold surface. In this paper we focused on short aromatic linker originating from thioacetate protected thiol functionalized fullerene. In contrary to free thiols which are readily oxidized, the thioesters are much more stable[7] and can be easily converted into thiols when needed.

Functionalization of gold nanoparticles (AuNPs) with C_{60} fullerene has been recently subject of a number of reports but usually alkyl thiols were employed[8-12] while aromatic moieties on the gold surface were attached to only indirectly.[13,14]

In the present paper, we describe the synthesis of a new C_{60} fullerene functionalized with a short aromatic thioacetate linker. Following deprotection, the fullerene derivative is used to self-assembly into densely packed fullerene layer on Au (111) surface of gold electrode or gold nanoparticles. Two variants, including the *in situ* procedure for the deprotection of the thioacetyl-derivatized fullerene by pyrrolidine were elaborated (Fig. 1). Both approaches can be of general interest because of their simplicity and lack of side reactions with the fullerene cage.

Electronic properties of the novel C_{60} derivative bound to both gold electrode and AuNPs were investigated using the electroanalytical methods. The gold nanoparticles showed narrow size distribution, well defined composition and high fullerene content, calculated to be ca. 30 fullerene substituents per single AuNP.

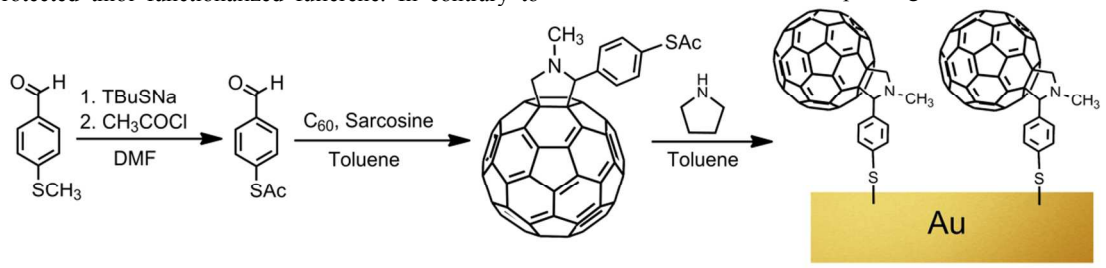

Fig. 1. Scheme for preparation of thioacetyl-functionalized C_{60} fullerene films on the gold surface.

RSC Advances Accepted Manuscript

Journal Name

RSCPublishing

ARTICLE

Experimental section

Reagents

Acetyl chloride, dimethylformamide (DMF) and pyrrolidine were obtained from Alfa Aesar. Hydrogen tetrachloroaurate(III), 4-(methylthio)benzaldehyde, sodium *tert*-butyl sulfide (*t*BuSNa), *N*-methylglycine, tetrabutylammoniumhexafluorophosphate (TBAHFP), tetraoctylammoniumbromide (TOAB) and toluene were bought from Sigma-Aldrich. Dichloromethane, ethanol, ethyl acetate, methanol, *n*-hexane, acetonitrile (AN) and sodium sulfate were purchased from POCh (Poland). Fullerene C_{60}, 99.9%, was obtained from MER Corp. DMF and toluene were dried and purified before use, according to standard procedures, other solvents were analytical grade reagents and were used as received.

Synthesis of fullerene thioacetate

4-(*S*-acethylthio)benzaldehyde was synthesized using the combination and modification of two methods described before.[15,16] To a suspension of *t*BuSNa (2.82 g; 25 mmol) in dry DMF (35mL), a solution of 4-(methylthio)benzaldehyde (1.9g; 12.5 mmol) in DMF (5 mL) was injected via a syringe while stirring vigorously. Reaction was kept under argon atmosphere at 153°C for 4h and suspension became dark brown. It was then cooled to 0°C and acetyl chloride (4.3mL; 60mmol) was added in strong Ar stream. After 45min, the resulting suspension was poured into 400 mL of water, followed by addition 80ml of CH_2Cl_2, resulting two phases were stirred for 30 min. and the organic layer was separated, extracted with water (2x10mL) and dried over anhydrous sodium sulfate. After evaporation of the solvent under reduced pressure the purification was accomplished by means of flash column chromatography (3:1 *n*-hexane: ethyl acetate) to give desired product as white solid.
Yield: 78%, mp 46°C, The mass spectrum (ESI-MS) showed a $[M+H]^+$ peak at 181.0 (Figure S1, Electronic Supplementary Information); IR (KBr disk) $\nu_{max}(cm^{-1})$ 2972.7, 2547.0, 1698.0, 1593.4, 1561.1, 1424.2, 1400.1, 1365.7, 1309.4, 1291.6, 1278.1, 1174.9, 1126.2, 1016.3, 941.1, 859.6, 810.4, 712.1, 625.3, 537.1 (Figure S5, Electronic Supplementary Information); ^{1}H NMR (200 MHz; $CDCl_3$; TMS) 2.47 (3H, s), 7.58-7.61 (2H, d, *J*=8.4Hz), 7.89-7.92 (2H, d, *J*=8.3Hz), 10.04 (1H, s) ppm (Figure S7, Electronic Supplementary Information); ^{13}C NMR (125 MHz; $CDCl_3$) 30.53, 130.02, 134.52, 135.44, 136.47, 191.46, 192.31 ppm (Figure S8, Electronic Supplementary Information).
Preparation of aromatic thioacetate functionalized C_{60} fullerene (**ATF-C_{60}**) was accomplished using the modified Prato synthesis.[17] A stirred solution of C_{60} fullerene (144 mg, 0.2mmol), 4-(S-acethylthio)benzaldehyde (36 mg, 0.2 mmol) and *N*-methylglycine (89 mg, 1mmol) in dry toluene (130 mL) was heated at reflux under argon atmosphere for 8 h. The reaction mixture was then cooled, filtered to remove insoluble precipitate and the solvent was removed under reduced pressure. The residue was chromatographed (2:1 *n*-hexane: toluene) to give pure **ATF-C_{60}** as dark brown powder.
Yield: 8%, the mass spectrum (ESI-MS) showed a $[M+Na]^+$ peak at 950.7 (Figure S2, Electronic Supplementary Information); IR (KBr disk) $\nu_{max}(cm^{-1})$ 2946.1, 2841.4, 2777.9, 1708.0, 1488.3, 1461.2, 1423.3, 1332.0, 1177.8, 1114.3, 1089.3, 1016.4, 944.6, 766.2, 728.0, 608.6, 552.4, 526.2, see (Figure S6, Electronic Supplementary Information); ^{1}H NMR (200 MHz; $CDCl_3$; TMS) 2.41 (3H, s), 2.83 (3H, s), 4.26-4.31 (1H, d, *J*=9.4Hz), 4.97 (1H, s), 4.97-5.02 (1H, d, *J*=10.1Hz), 7.46-7.51 (2H, d, *J*=8.5Hz), 7.88-7.93 (2H, d, *J*=7.4Hz) ppm (Figure S9, Electronic Supplementary Information);^{13}C NMR (125 MHz; $CDCl_3$) 30.30, 40.29, 69.19, 70.14, 83.02, 128.17, 135.70, 135.96, 138.58, 139.93, 141.90, 140.02, 140.05, 142.07, 142.12, 142.16, 142.26, 142.60, 144.43, 145.21, 145.30, 145.34, 145.37, 145.56, 145.57, 145.97, 145.99, 146.17, 146.31, 147.34, 152.92, 153.10, 153.94, 156.11, 193.93 ppm (Figure S10, Electronic Supplementary Information).

Deprotection of fullerene thioacetate

At the very beginning we discarded reported sodium hydroxide[18] and sodium thiomethoxide[19] methods that required use of ethanol and methanol respectively, solvents which synthesized fullerene compound was insoluble in. However, aromatic thioacetate group present in some non-relalated compounds was previously deprotected also in solvents suitable for most fullerene derivatives using tetrabutylammonium hydroxide (TBAH)[20] or aliphatic amines, i.e. triethylamine,[20,21]. Seemingly, synthesized fullerene thioacetate should follow the same route. Unexpectedly, we observed difficulties that turned out to be inherent to aromatic tioacetate fullerene derivatives while trying to apply these common deprotection procedures. Despite good solubility of fullerene thioacetate in tetrahydrofuran the use of TBAH solution was unable to deprotect **ATF-C_{60}** because brown precipitate formed soon after addition of tetrabytulammonium hydroxide solution. The probable explanation for this fact can be that TBAH is well known catalyst of fullerene hydroxylation[22] and some insoluble fullerenol was formed instead of desired free thiol. The second studied deprotection agent was triethylamine;[20,21] which can also react with C_{60} fullerene as reported previously by Kajii et al.[23] and in our case even large excess of Et_3N in toluene did not deprotect **ATF-C_{60}** to form free thiol. After that, we tried to use a modified procedure given by Yelm[24] who applied pyrrolidine to deprotect non-fullerene aromatic thioacetates in solvents suitable for fulleropyrrolidines. Despite the fact that fulleropyrrolidines are less reactive than pure C_{60} fullerene[25] we were still considering possible side-reactions of pyrrolidine with C_{60} fullerene cage under aerobic conditions[26,27] and the chance that heat also may promote reaction of secondary amines with fullerene,[28] so the deprotection was finally done under inert gas atmosphere and without heating. This time results were fully satisfying, thiolate anion of deprotected ATF-C_{60} has been detected by means of ESI-MS (Figure S3, Electronic Supplementary Information). Thus, pyrrolidine at room temperature and in inert gas atmosphere was found to be the best deprotection agent for synthesized fullerene

RSC Advances Accepted Manuscript

thioacetate. However, *in situ* deprotection with gold plate immersed into a solution of **ATF-C_{60}** with 20eq. of pyrrolidine led to formation of multilayer with remaining traces of amine whereas removal of the pyrrolidine excess before self-assembly allowed producing stable monolayers on both gold electrode and nanoparticles. In typical procedure to a 0.5mM solution of **ATF-C_{60}** in toluene (10mL) 7.1 mg (8.3μL, 0.1mmol) of pyrrolidine was added. Resulting mixture was stirred for 3h at room temperature under argon atmosphere. Then, mixture was concentrated under reduced pressure, removing the pyrrolidine at the same time, and 10 mL of methanol was added. Precipitate was centrifuged (10 000 rpm, 5 min), washed with methanol and monitored by TLC and ESI-MS for complete removal of formed N-acetylpyrrolidine (detected in methanol solution by ESI-MS, see Figure S4, Electronic Supplementary Information) and any remaining traces of pyrrolidine (usually not present in supernatant). Then it was dissolved in 10ml of toluene to form stock solution **S** and proceeded to self-assembly.

Self-assembly of thioacetate derivative on surface of gold electrode

Attempts to obtain self-assembled monolayer (SAM) of fullerene thioacetate at the gold electrode surface without previous deprotection procedure failed, so we can assume that from the mixture of deprotected fullerene derivative and fullerene thioacetate only the first one should deposit on Au surface. Self-assembly of deprotected **ATF-C_{60}** on gold electrode was done by dipping the gold substrates into the solution **S** diluted 100x with toluene or 1,2,4-trichlorobenzene for 24h at RT. Resulting films were washed with the corresponding solvent and dried under stream of nitrogen. After successful approach with chemisorption of C_{60} derivative on the surface of gold electrode we decided to synthesize gold nanoparticles covered with C_{60} using deprotected fullerene thioacetate as a ligand.

Synthesis of gold nanoparticles

Gold NPs were prepared using a modified Brust-Schiffrin method reaction.[29] An aqueous solution of hydrogen tetrachloroaurate (III) (30 mL, 30 mM) was extracted with 80 mL of tetraoctylammonium bromide (2.19 g, 4 mmol) solution in toluene. Most of the tetrachloroaurate ions were transferred to the organic layer as the yellow aqueous layer faded until colorless. 1.44 μL ($8.3 \cdot 10^{-6}$M) of 1-octanethiol was added to the organic phase, and the mixture was reduced with freshly prepared aqueous solution of sodium borohydride (378mg, 200 mmol in 25 mL of deionized water). A solution of borohydride was very slowly added under vigorous stirring. After further stirring for 3 h, the organic phase was separated, evaporated to 10 mL in a rotary evaporator, and mixed with 400 mL of absolute ethanol to precipitate NPs. The mixture was kept for 12 h at -4 °C. The dark brown precipitate was sonicated for 60 s and centrifuged (5 min, 13 000 rpm). Again, the precipitate was dissolved in a small amount of toluene (10 mL), precipitated with ethanol (400 mL), and centrifuged. Finally, all samples were dissolved in 10 mL of toluene. Obtained nanoparticles were characterized by TEM, UV-Vis and DLS measurements.

AuNPs Ligand-Exchange Reaction

An organic ligand deprotected **ATF-C_{60}** toluene solution **S** (10mL) was added to the toluene solution of octanethiol stabilized gold NPs (200 μL), and the reaction proceeded for ca. 72 h upon mixing at room temperature. As no precipitation and/or color change occurred, we inferred that this ligand-exchange reaction was not accompanied by side effects, such as irreversible aggregation or significant gold core size modifications. The clear burgundy solution was rotary evaporated, and the blackish solid was dissolved in a small volume of toluene (max. 2 mL). In the next step, the NPs were precipitated using ethanol and centrifuged 2 h later (13 000 rpm, 5 min). The precipitate was dissolved in toluene, sonicated and the suspension was centrifuged again at 13 000 rpm for 20 minutes The toluene washing process was repeated several times until the supernatant fluid became colorless. Resulting fullerene functionalized nanoparticles were characterized by UV-Vis, DLS and XPS measurements.

Characterization methods and Instrumentation

ESI-MS spectra were acquired on a Micromass LCT ESI-TOF mass spectrometer equipped with an orthogonal electrospray ionization source. ^{1}H NMR and ^{13}C NMR spectra were recorded on Varian Unity Plus 200 and 500 MHz spectrometers, respectively, using $CDCl_3$ as a solvent. The infrared experiments were carried out using the Nicolet 8700.

XPS measurements were carried out using a VG ESCALAB 210 electron spectrometer equipped with an Al Kα source (1486.6 eV). XPS data were calibrated using the binding energy of C1s 285.0 eV as the internal standard.

The morphology and size of obtained gold nanoparticles were obtained using a Libra TEM (Carl Zeiss) operating at 120 kV.

UV-Vis spectra were collected from 300 to 700 nm using Evolution 60 UV-Vis Spectrophotometer from Thermo Scientific and a quartz glass cuvette.

The Dynamic Light Scattering (DLS) measurements were performed using Zetasizer Nano ZS from Malvern Instruments.

Thermogravimetric analysis (TG) was performed under high purity nitrogen atmosphere using TA Instruments Q50 Thermal Gravimetric Analyzer with heating rate of 5K/min.

CV (Cyclic Voltammetry) and DPV (Differential Pulse Voltammetry) experiments were done using the Autolab potentiostat (ECO Chemie, Netherlands) in a three electrode arrangement, with a silver/silver chloride (Ag/AgCl) electrode as the reference, platinum foil as the counter and the glassy carbon electrode (GCE, BAS, 3mm diameter) or the modified gold electrodes (gold (200nm) evaporated on glass with a pre-layer of 2-4 nm of chromium (Gold Arrandee, Gmbh) as the working electrodes. The reference electrode was separated from the working solution by an electrolytic bridge filled with 0.1M TBAHFP/toluene/AN (4:1) solution. The reference potential electrode was calibrated using the ferrocene (Fc) redox process in the same TBAHFP/toluene/AN solution, which was also used as the supporting electrolyte. Argon was used to deaerate solution and an argon blanket was maintained over the solution during the experiments. All experiments were carried out at 25°C.

The Atomic Force Microscopy (AFM) images were acquired using Agilent Technologies 5500AFM (Agilent Technologies, Santa Clara, CA, USA). The non-contact mode was used for imaging. Ultra sharp probes were purchased from NANOSENSORS (SSS-NCLR with 2 nm tip radius). Single gold monocrystal was applied as substrate for AFM measurements. The atomic flat Au (111) surface at monocrystal surface was used for image acquisition. Substrate before fullerene adsorption and AFM imaging was flame annealed and cleaned in piranha solution (concentrated H_2SO_4/30% H_2O_2 3:1 v/v) for 30 minutes and rinsed with Milli-Q ultrapure water. AFM images of fullerene derivative-modified Au substrate were recorded after its immersion in fullerene solutions for 24 hours.

RSC Advances Accepted Manuscript

Results and discussion

TEM measurements

One or two droplets of as-prepared nanoparticle solutions diluted with toluene to a very small concentration were placed on a standard copper grid (400-mesh) coated with carbon. The grid was left overnight to dry. The TEM image of the synthesized AuNPs is shown in Fig. 2. The dispersed nanoparticles have an average diameter of 4.72 nm.

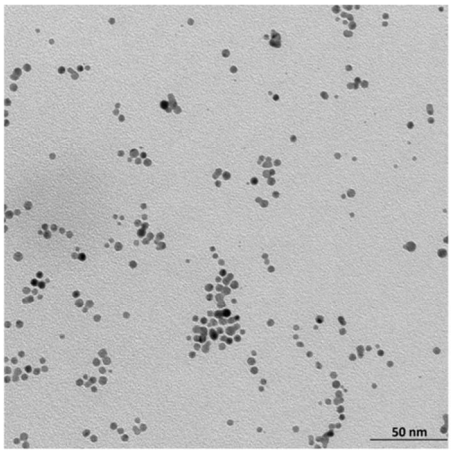

Fig. 2. TEM image of AuNPs with average size of 4.72 nm obtained at 120 kV.

UV-Vis Spectroscopy

UV-Vis spectroscopy was used to control the formation of **ATF-C_{60}-AuNPs** by observation of a peak referring to the maximum of absorption at 522 nm. Data were collected from 300 to 700 nm for 3 different species: the starting solution of AuNPs (20 µL of NPs diluted 40x with toluene), the solution of gold nanoparticles modified with fullerene derivative (250 µL of modified NPs diluted 3.2x with toluene) and **ATF-C_{60}** solution in toluene (C = 0.0176 mg/mL). As we can observe in Fig. 3. fullerene functionalized nanoparticles retain peak coming from AuNPs-octanethiol (λ_{max} = 522 nm) and show additional one referring to the maximum of absorption at 336 nm for C_{60} derivative **ATF-C_{60}** indicating the successful exchange of the ligand.[12]

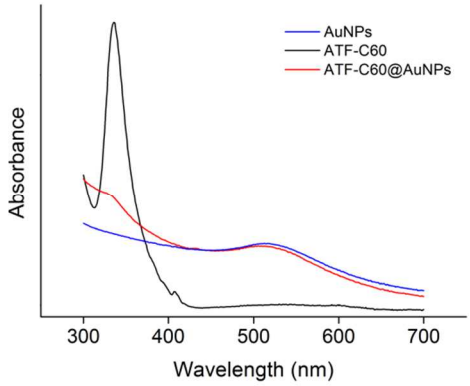

Fig. 3. UV-Vis spectra of bare octanethiol AuNPs, **ATF-C_{60}** and **ATF-C_{60}@AuNPs** collected from 300 to 700 nm.

Dynamic Light Scattering

Size of single fullerene thioacetate molecule was theoretically estimated from fully optimized geometry structure using the DFT/B3LYP/6-31g*,[30-33] approach to be 1.37nm. Dynamic Light Scattering measurements (Figure S11, Electronic Supplementary Information) sized the bare octanethiol-AuNPs as 4.71nm which is in excellent agreement with TEM results (4.72nm). AuNPs coated with fullerene derivative indicated the average diameter of 7.27nm (Figure S12, Electronic Supplementary Information). Substracting the size of fullerene coating which increases the whole size of nanoparticle by 2.74nm, the average size of coated nanoparticle can be assessed to be 4.53nm, thus slightly less than that from DLS measurements. This induces that we clearly obtain a monolayer and the orientation of fullerene substituents is probably not perpendicular to the AuNP surface but slightly tilted from the surface normal.

FTIR spectroscopy of SAMs

Fig. 4. shows FTIR spectra of both **ATF-C_{60}** and its deprotected SAMs on the surface of gold electrode. Deprotection of **ATF-C_{60}** and its deposition on Au surface causes several changes in the infrared spectrum. The intense signal at 1708 cm^{-1} attached to the C=O stretching mode almost completely disappeared confirming the efficient deprotection of thioacethyl group and removal of N-acetylpyrrolidine. Four characteristic fulleropyrrolidine bands are visible in both spectra and their positions are similar. Bands at 1113-1114 cm^{-1} and 1423-1424 cm^{-1} are associated with C_{60} fullerene cage and contribution of pyrrolidine ring is visible in the range of 2750-3000 cm^{-1}.[34]

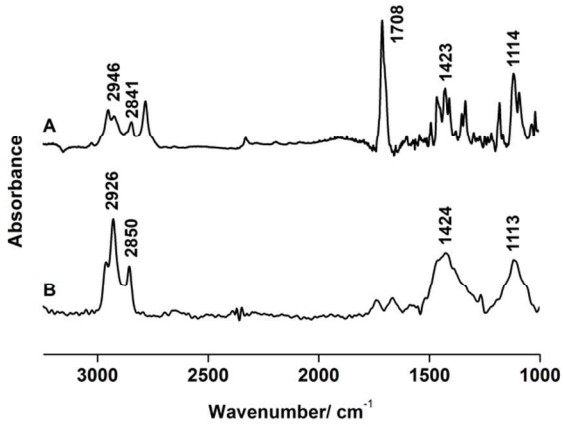

Fig. 4. IR spectra of **ATF-C_{60}** in KBr pellet (A) and the reflectance spectrum of the thin film obtained after its deprotection and self-assembly from solution **S** diluted 100x with 1,2,4-trichlorobenzene (B).

Atomic Force Microscopy

The surface morphology of deprotected **ATF-C_{60}** layer deposited, on the Au(111) surface, from pyrrolidine free solution **S** diluted 100x

RSC Advances Accepted Manuscript

This journal is © The Royal Society of Chemistry 2012

with two different solvents: 1,2,4-trichlorobenzene (Fig.5A) and toluene (Fig.5B) was studied by AFM. Both images provide a precise insight into the surface morphology and allow for assessing the influence of the solvents used for the self-assembly on the topography of the films of deprotected thiolated fullerene derivatives deposited on gold. In both cases, the gold surface is covered by small granular aggregates. Analysis of the AFM images enables us to evaluate the average size of these grains. Diameter of the smallest fullerene aggregates was estimated to be in the range of 65-80 nm in the case of toluene and 10-15 nm for 1,2,4-trichlorobenzene. In addition, there are more morphological differences between the films obtained in toluene and trichlorobenzene solutions. Namely, the aggregated grains in the Figure 5B have no clearly marked spherical shapes and exhibit a tendency to form large domains with diameters up to ca. 200 nm which are visible as bright spots. Comparing images in Figure 5A and 5B it is obvious that the morphology of fullerene aggregates depends strongly on the solvent properties. Smaller fullerene grains obtained in case of 1,2,4-trichlorobenzene solution are not surprising, considering dielectric constant, ε of each solvent and the higher solubility of fullerene derivatives in 1,2,4-trichlorobenzene,[35] both factors favor the formation of smaller aggregates[36] as clearly demonstrated in the presented figures. Obtained AFM results confirm earlier reports that fullerene derivatives can not self-assemble into ordered monomolecular layers.[37,38]

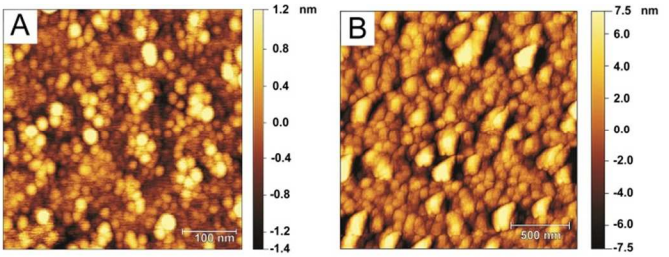

Fig. 5. Non-contact AFM images of self-assembled films of deprotected **ATF-C_{60}** on Au(111) from solution **S** diluted 100x with A) 1,2,4-trichlorobenzene, B) toluene.

XPS Spectroscopy Results

X-ray photoelectron spectroscopy was used to assess the composition of nanomaterials obtained from self-assembly of *in situ* deprotected thioacetate, chemisorption after removal of pyrrolidine and N-acetyl pyrrolidine as well as of nanoparticles functionalized with C_{60} fullerenes. XPS spectra of all investigated samples show the presence of gold, sulfur, nitrogen, carbon while the nanoparticles sample also contained bromine atoms. Binding energies obtained from XPS spectrum confirmed the presence of functionalized fullerenes on the surface of gold electrode and gold nanoparticles attached to Au by the sulfur atoms.

The S2p region of spectrum obtained for the *in situ* deprotection sample (Fig. 6A) shows two doublets, each with area ratios of 2:1 and splitting of 1.2 eV. First one is observed at 161.9 eV and 163.1 eV assigned to $S2p_{3/2}$ and $S2p_{1/2}$ respectively, this binding energy value is typical for the S–Au bond[39] and it was found to be 53 at% of all sulfur atoms in the sample. Second doublet at 163.8 eV for $S2p_{3/2}$ and 165.0 eV for $S2p_{1/2}$ corresponds to surface unbound sulfur atoms[7] and equals remaining 47 at%. These results are in good agreement with AFM data suggesting that the proposed *in situ* method results in thick multilayer formation.

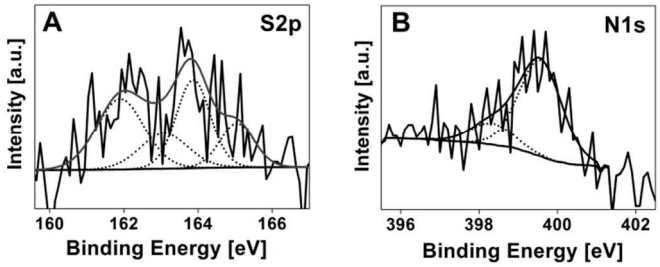

Fig. 6. Partial XPS spectra of the S2p and N1s regions for films obtained using *in situ* **ATF-C_{60}** deprotection method.

Results for the N1s region were deconvoluted into two peaks (Fig. 6B). According to literature data the bigger one observed at 399.7 eV is assigned to nitrogen atoms from fulleropyrrolidine[40] with atomic percent value of 81 at%. Second peak with the lower binding energy of 398.4 eV is assigned to pyrrolidine[41], indicating that amine remains in obtained film (19 at%). However, taking into account the small molecular mass of pyrrolidine in comparison to the functionalized fullerene molecule the overall weight percent of both components are 98 wt% for fullerpyrrolidine and only 2 wt% for pyrrolidine. These results show that *in situ* deprotection of aromatic thioacetate can be used whenever the thickness of the film and remaining small amount of amine still meet application requirements.

In the S2p region of the XPS spectra of the thin film obtained using pyrrolidine free solution **S** of deprotected **ATF-C_{60}** dilluted 100x with 1,2,4-trichlorobenzene (Fig. 7A) one doublet at 161.9eV and 163.1eV is observed, with expected 2:1 ratio. This results show that all sulfur atoms in the investigated sample are bound to gold surface.

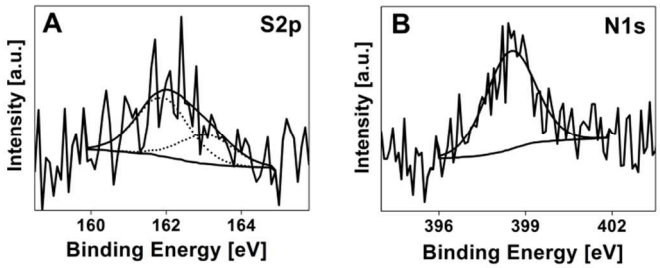

Fig. 7. Partial XPS spectra of the S2p and N1s regions for films obtained using pyrrolidine free solution of deprotected **ATF-C_{60}**. $S2p_{3/2}$:$S2p_{1/2}$ intensity ratio 2:1 and splitting of 1.2 eV.

The N1s photoelectron peak appears at 399.8eV (Fig. 7B) and we can assign it to the fulleropyrrolidine nitrogen atoms. As a result, the pyrrolidine free mixture lead to deposition of functionalized fullerenes without any impurities and formation of thin film on the gold electrode surface.

Results obtained for AuNPs covered with functionalized fullerenes reveal a doublet in the S2p region (Fig. 8A) (2.0 at% overall atoms). It was deconvoluted into two peaks centered at 162.0 and 163.2eV corresponding to $S2p_{3/2}$ and $S2p_{1/2}$ atoms, confirming that all **ATF-C_{60}** molecules are bound to the surface of gold nanoparticles by S-Au bonds and, no fullerene-gold interaction is observed. A double-peak observed in the N1s scanning range (Fig. 8B) from 396 to 404 eV was deconvoluted with very good correlation in two peaks with binding energies 399.3 eV and 402.1 eV associated with fulleropyrrolidine and quaternary ammonium nitrogen[42] respectively

RSC Advances Accepted Manuscript

(38 at% and 62 at% of all nitrogen atoms, 0.8 at% and 1.3 at% overall atoms). XPS spectrum of the Br3d region confirms the presence of bromine from tetraoctylammonium salt with intensity 1.1 at% overall atoms which is in good correlation with results obtained for their counter tetrabutylammonium ion nitrogen atoms (1.3%). Results presented above allow to calculate **ATF-C$_{60}$** : TOAB: octanethiol ratio on AuNPs surface from corresponding signals (0.8at%: 1.3at%: (2% of total S amount - 0.8 at% S from **ATF-C$_{60}$**)), that is exactly 1:1.625:1.5.

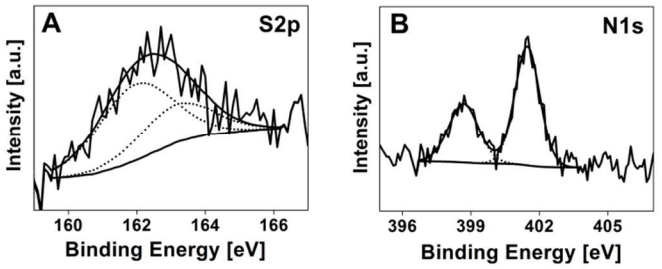

Fig. 8. Partial XPS spectra of the S2p and N1s regions for gold nanoparticles functionalized with deprotected **ATF-C$_{60}$**.

In summary, thioacetate group is not observed according to XPS results for all samples, which is confirmed by lack of S2p$_{3/2}$ signal at around 163.eV, typical for S-C bond.[43,44]. Thus confirming the efficiency of deprotection and selective deposition of free thiol instead of S-acetyl functionalized fullerene from any remaining traces of protected compound. Moreover, the absence of peaks above 166 eV for S2p region indicates that the obtained fullerene-gold nanocomposites are free from oxidized sulfur species usually found at higher binding energies.[45]

Thermogravimetric analysis

TG analysis results (Fig. 9.) showed that 8.5% of total mass of nanoparticles is organic coating and remaining 91.5% was clearly visible pure Au. Assuming the spherical shape of nanoparticles, the average number of gold atoms per AuNP (N_{Au}) was calculated according to Eq. (1) proposed by Huo et al.[46] whereas the number of fullerene ligands per nanoparticle (N_L) was determined using XPS results by Eq. (2) (where $\%wt_{org}$ and $\%wt_{Au}$ are thermogravimetrically determined percentage mass values for organic coating and Au core respectively, D is the average diameter of AuNPs in nm, M_L and M_{oct} are molecular masses of corresponding **ATF-C$_{60}$** and octanethiol thiolate anions, M_{Au} is atomic weight of gold and M_{TOAB} stands for the molecular mass of tetraoctylammonium bromide) and was found to be ca. 30. The remaining organic mass at the AuNP surface consists of tetraoctylammonium ions and octanethiol molecules. Note, that the left factor in the Eq. (2) corresponds to the total mass of organic coating and the right one is connected to the fullerene content.

$$N_{Au} = 30.89602D^3 \quad (1)$$

$$N_L = \frac{\%wt_{org} \cdot M_{Au} \cdot 30.89602D^3}{\%wt_{Au}} \cdot \frac{1}{1 \cdot M_L + 1.625 \cdot M_{TOAB} + 1.5 \cdot M_{oct}} \quad (2)$$

$$N_L = \frac{8.5 \cdot 197.0 \cdot 30.89602 \cdot 4.72^3}{91.5} \cdot \frac{1}{1 \cdot 884.9 + 1.625 \cdot 546.7 + 1.5 \cdot 145.3}$$

$$N_F = 29.86$$

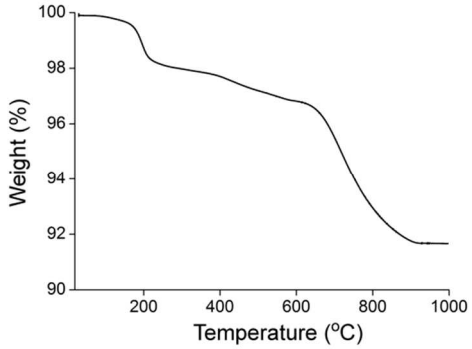

Fig. 9. Results of TG analysis obtained for the AuNPs covered with deprotected **ATF-C$_{60}$**.

Electrochemical behavior of thioacetate derivative in the solution

Electrochemical properties of C_{60} and thioacetate derivative **ATF-C$_{60}$** in 0.1M TBAHFP toluene/acetonitrile solution were investigated using voltammetry (CV and DPV). The fullerene moiety preserves sequential one-electron reversible redox processes characteristic of the extended π-electron system (Fig.10 A).[1,47] The one-to-one ratio of CV peak currents and the close to 60 mV peak-to-peak separation confirm the reversibility. The thioacetate derivative exhibits the voltammetric behavior similar to that of C_{60}, however, the peak potentials are shifted to more negative values due to the presence of linker, and the peak currents are much smaller indicating smaller diffusion coefficients of the derivative compared to that of unmodified fullerene.

Four reversible peaks were also recorded in the DPV experiment. The fullerene centered processes appear again at more negative potentials, compared to of C_{60} (Fig. 10B). Such shifts are due to the presence of a substituent containing an electron donating moiety, in this case the aromatic ring. As the result, the fullerene derivative becomes a weaker electron acceptor than the unsubstituted molecule, however the reversibility of each of the first 4 steps of the electrode processes is retained. All peak currents of the thioacetate derivative are smaller than those of the unsubstituted fullerene reflecting the smaller diffusion coefficients - the molecule is larger due to the presence of the substituent.

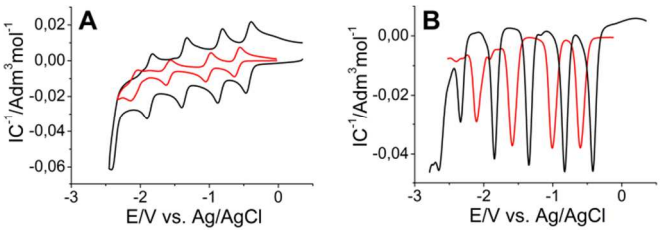

Fig. 10. Voltammograms of (black line) C_{60} and (red line) compound **ATF-C$_{60}$** in 0.1 M TBAHFP/ toluene/acetonitrile (4:1), (A) CV, v = 100 mV/s; (B) DPV, tp= 3 ms, ΔE = 50 mV (characteristic parameters of the voltammetric behavior of

RSC Advances Accepted Manuscript

This journal is © The Royal Society of Chemistry 2012

compound **ATF-C_{60}** are given in Electronic Supplementary Information Table S1).

Application of deprotected thioacetate derivative ATF-C_{60} for Au electrode and AuNPs modification

The C_{60} thioacetate derivative following its deprotection was self-assembled on the gold electrode surface. The cyclic voltammogram of the gold electrode modified with self-assembled monolayer of C_{60} derivative recorded in acetonitrile containing 0.1M TBAHFP is shown on Fig.11 (A).

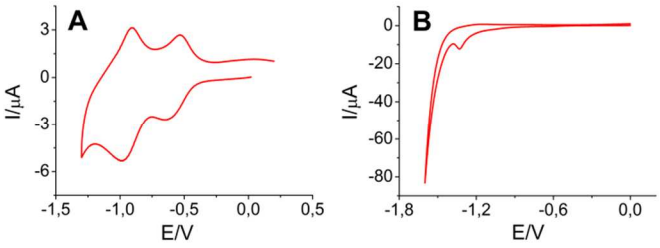

Fig. 11. Cyclic voltammogram of deprotected C_{60} derivative **ATF-C_{60}** (A) self-assembled monolayer recorded in 0.1 M TBAHFP solution in AN, v = 1V/s and (B) desorption of adsorbed monolayer in 0.5M KOH in water, v=50mV/s.

The two redox peaks observed in Figure 11A, correspond to the first and second redox step of the immobilized fullerene derivatives. The redox potentials are close to the values reported for fullerene lipoic acid derivative or fullerene with long alkane thiol chain self-assembled on the gold substrates.[48,49] The peak currents increase linearly with scan rate as predicted for the surface immobilized species. The surface concentration of the deprotected **ATF-C_{60}** derivative was calculated based on Eq. (3):

$$\Gamma = Q/nFA \qquad (3)$$

where n is the number of exchanged electrons, A is the electrode surface area in cm^2, Γ is the surface concentration in mol cm^{-2}, Q is the charge under the peak in C. The surface concentration of the fullerene is $7.1 \cdot 10^{-11}$ mol cm^{-2}.

Γ_{CV} is calculated from the charge of the fullerene reduction peak while Γ_{des} is obtained from the charge of the reductive desorption peak of the compound from the Au surface. Assuming that fullerene occupies on the surface ca. 95Å^2, the surface concentration should be $1.75 \cdot 10^{-10}$ mol cm^{-2}. The surface concentration Γ_{des} is slightly smaller ($8.3 \cdot 10^{-11}$ mol cm^{-2}) than the value corresponding to a monolayer. The values of Γ_{CV} are similar to those of Γ_{des}.

Figure 12 compares the cyclic voltammograms of **ATF-C_{60}** and of the tethered gold nanoparticles, **ATF-C_{60}@AuNPs**. It can be seen that there are four pairs of voltammetric waves for the **ATF-C_{60}** solution (red curve), which are all close to reversible. For the **ATF-C_{60}@AuNPs**, a series of two well-defined voltammetric peaks at -0.56 and -0.95V can be found within the potential range of -1.4 to 0V. These signals can be ascribed to the successive 1ē reduction steps of the C_{60} molecules, i.e., $C_{60}^{0/-1}$ and $C_{60}^{-1/-2}$ couples, respectively.[47,50,51] The capacitance is much larger for the **ATF-C_{60}@AuNPs** compared to the faradaic process. Interestingly the shift of peak potentials indicates stronger electron acceptor properties of the fullerenes when bound to gold nanoparticles compared to those of **ATF-C_{60}** dissolved in the solution. The dependence of peak current versus $v^{1/2}$ in both cases **ATF-C_{60}@AuNPs** and pure fullerene derivative is linear with $R^2 = 0.982$ and 0.991, respectively (Figure 13). It indicates that the process is controlled by diffusion.

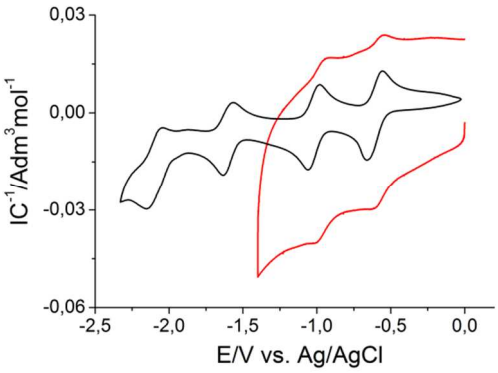

Fig. 12. Voltammograms of (black line) **ATF-C_{60}** and (red line) the C_{60} derivative tethered gold nanoparticles (**ATF-C_{60}@AuNPs**) in solution 0.1 M TBAHFP/ toluene/acetonitrile (4:1), CV, v=100 mV/s.

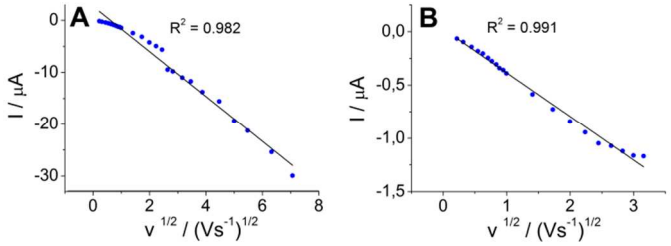

Fig. 13. Dependence of peak current versus $v^{1/2}$ for **ATF-C_{60}@AuNPs** (A) and the fullerene derivative **ATF-C_{60}** in a solution 0.1 M TBAHFP/ toluene/acetonitrile (4:1) (B).

Conclusions

A new procedure for efficient modifiction of gold surfaces with fullerenes has been elaborated. Firstly, a new aromatic thioacetate functionalized fullerene derivative **ATF-C_{60}** was synthesized in a two step procedure and was thoroughly characterized using a wide range of analytical techniques. The electrochemical behavior of the thioacetate functionalized fullerene derivative was evaluated in toluene/acetonitrile solution and 4 reversible sequential 1e electrode processes were resolved both in the cyclic and differential pulse voltammograms

In the next step, the newly synthesized molecules following suitable deprotection, were used for the preparation of the C_{60} fullerene–modified gold electrode, and C_{60} fullerene-modified gold nanoparticles. The proposed deprotection procedure for S-acetyl-derivatized aromatic fullerene is very efficient and allows the control of the thickness of the self-assembled fullerene layer providing complete removal of the excessive pyrrolidine and resulting N-acetylpyrrolidine. Otherwise, traces of the deprotection reagents can promote multilayer formation as found from the XPS data.

The described two-step approach proved to be an efficient way for the preparation of fullerene modified gold nanoparticles. Interestingly, the gold nanoparticles coverage is higher than achieved using one-step procedures. DLS and TEM measurements

RSC Advances Accepted Manuscript

show that octanethiol-AuNPs of 4.71nm diameter following ligand exchange procedure gave fullerene modified AuNPs of 7.27nm diameter with high population of 30 bound fullerene moieties per one nanoparticle. Anchoring the fullerene on gold nanoparticle lead also to improved acceptor properties of the fullerene moieties that was confirmed by easier uptake of electrons from the electrode in the electrochemical experiments.

Acknowledgements

We gratefully acknowledge the financial support from the National Science Centre (Projects: Piotr Piotrowski 2012/07/N/ST5/01966 and Joanna Pawłowska 2011/03/N/ST5/04825). Theoretical calculations were performed using the computational resources of the Interdisciplinary Center for Mathematical and Computational Modeling at Warsaw University (Grant G15-11).

Notes and references

[a] Department of Chemistry, University of Warsaw, Pasteura 1, 02-093 Warsaw, Poland.

[b] Faculty of Chemistry, Biological and Chemical Research Centre, University of Warsaw
Żwirki i Wigury 101, 02-089 Warsaw, Poland.

† Electronic Supplementary Information (ESI) available: Additional characterization data including ESI-MS, IR and ^{1}H NMR spectra for synthesized coumpounds and dynamic light scattering (DLS) data are presented. See DOI: 10.1039/b000000x/

1 L. Echegoyen and L.E. Echegoyen, *Acc. Chem. Res.*, 1998, **31**, 593-601.
2 D. Bonifazi, O. Enger and F. Diederich, *Chem. Soc. Rev.*, 2007, **36**, 390-414.
3 S. Urnikaite, T. Malinauskas, V. Gaidelis, R. Maldzius, V. Jankauskas and V. Getautis, *Carbon* 2011, **49**, 320-325.
4 E. Busseron, Y. Ruff, E. Moulin and N. Giuseppone, *Nanoscale*, 2013, **5**, 7098-7140.
5 Y. Matsuo, S. Lacher, A. Sakamoto, K. Matsuo and E. Nakamura, *J. Phys. Chem. C*, 2010, **114**, 17741-17752.
6 Q. Xu, H. Ma, H. Yip and A.K. Jen, *Nanotechnology*, 2008, **19**, 135605.
7 Y. Shirai, L. Cheng, B. Chen and J.M. Tour, *J. Am. Chem. Soc.*, 2006, **128**, 13479-13489.
8 H. Fujihara and H. Nakai, *Langmuir*, 2001, **17**, 6393-6396.
9 P.K. Sudeep, B.I. Ipe, K.G. Thomas and M.V. George, *NanoLett.*, 2002, **2**, 29-35.
10 R. Rashimi and A. Patnaik, *Journal of Colloid and Interface Science*, 2003, **268**, 43-49.
11 F. Lu, S. Xiao, Y. Li, Y. Song, H. Liu, H. Li, J. Zhuang, Y. Liu, L. Gan and D. Zhu, *Inorg. Chem. Comunm.*, 2004, **7**, 960-962.
12 F. Deng, Y. Yang, S. Hwang, Y-S. Shon and S. Chen, *Anal. Chem.*, 2004, **76**, 6102-6107.
13 Y-S. Shon and H. Choo, *Chem. Commun.*, 2002, 2560-2561.
14 M. Geng, Y. Zhang, Q. Huang, B. Zhang, Q. Li, W. Li and J. Li, *Carbon*, 2010, **48**, 3570-3574.
15 D.T. Gryko, C. Clausen and J.S. Lindsey, *J. Org. Chem.*, 1999, **64**, 8635-8647.
16 A. Pinchart, C. Dallaire and M. Gingras, *Tetrahedron Lett.*, 1998, **39**, 543-546.
17 M. Prato and M. Maggini, *Acc. Chem. Res.*, 1998, **31**, 519-526.
18 A. Van den Hoogenband, J.H.M. Lange, R.P.J. Bronger, A.R. Stoit and J.W. Terpstra, *Tetrahedron Lett.* 2010, **51**, 6877-6881.
19 Wallace, O.B.; Springer, D. M. Mild, *Tetrahedron Lett.* 1998, **39**, 2693–2694.
20 H. Valkenier, E.H. Huisman, P.A. van Hal, D.M. de Leeuw, R.C. Chiechi and J.C. Hummelen, *J. Am. Chem. Soc.*, 2011, **133**, 4930-4939.
21 A. Shaporenko, M. Elbing, A. Blaszczyk, C. von Hanisch, M. Mayor and M. Zharnikov, *J. Phys. Chem. B*, 2006, **110**, 4307–4317.
22 K. Kokubo, S. Shirakawa, N. Kobayashi, H. Aoshima and T. Oshima, *Nano Research* 2011, **4**, 204-215.
23 Y. Kajii, K. Takeda and S. Shibuya, *Chem. Phys. Lett.* 1993, **204**, 283-286.
24 K.E. Yelm, *Tetrahedron Lett.*, 1999, **40**, 1101-1102.
25 N. Martín, M. Altable, S. Filippone, A. Martín-Domenech, L. Echegoyen and C.M. Cardona, *Angew. Chem. Int. Ed.*, 2005, **45**, 110-114.
26 H. Isobe, N. Tomita and E. Nakamure, *Org. Lett.*, 2000, **2**, 3663-3665.
27 G. Schick, K-D. Kampe and A. Hirsch, *J. Chem. Soc., Chem. Commun.*, 1995, 2023-2024.
28 U. Dzhemilev, A. Ibragimov, A. Tuktarov, V. D'yakonov, M. Pudas and U. Bergmann, *Russ. J. Org. Chem.*, 2007, **43**, 375-379.
29 M. Brust, M. Walker, D. Bethell, D.J. Schiffrin and R. Whyman, *J. Chem. Soc., Chem. Commun.*, 1994, 801-802.
30 A.D Becke, *J. Chem. Phys.*, 1993, **98**, 5648-5652
31 C. Lee, W. Yang and R.G. Parr, *Phys. Rev. B*, 1988, **37**, 785-789.
32 P.C. Hariharan and J.A. Pople, *Theor. Chim. Acta*, 1973, **28**, 213-222.
33 W.J. Hehre, R. Ditchfield and J.A. Pople, *J. Chem. Phys*. 1972, **56**, 2257-2261.
34 H. Imahori, S. Kitaura, A. Kira, H. Hayashi, M. Nishi, K. Hirao, S. Isoda, M. Tsujimoto, M. Takano, Z. Zhe, Y. Miyato, K. Noda, K.. Matsushige, K. Stranius, N.V. Tkachenko, H. Lemmetyinen, L. Qin, S.J. Hurst and C.A. Mirkin, *J. Phys. Chem. Lett.*, 2012, **3**, 478-481.
35 R.S. Ruoff, D.S. Tse, R. Malhorta and D.C. Lorents, *J. Phys. Chem.*, 1993, **97**, 3379-3383.
36 T. Rudalevige, A. Francis and R. Zand, *J. Phys. Chem. A* 1998, **102**, 9797-9802.
37 C.C. Chu, G. Raffy, D. Ray, A. Del Guerzo, B. Kauffmann, G. Wantz, L. Hirsch and D.M. Bassani, *J. Am. Chem. Soc.*, 2010, **132**, 12717-12723.
38 P. Piotrowski, J. Pawłowska, J. Pawłowski, A. Więckowska, R. Bilewicz and A. Kaim, *J. Mater. Chem. A*, 2014, **2**, 2353-2362.
39 N. Crivillers, Y. Takano, Y. Matsumoto, J. Casado-Montenegro, M. Mas-Torrent, C. Rovira, T. Akasaka and J. Veciana, *Chem. Commun.*, 2013, **49**, 8145.

RSC Advances Accepted Manuscript

 This journal is © The Royal Society of Chemistry 2012

40 D. Benne, E. Maccallini, P. Rudolf, C. Sooambar and M. Prato, *Carbon*, 2006, **44**, 2896-2903.
41 H. Liu and R.J. Hamers, *Surf. Sci.*, 1998, **416**, 354-362.
42 S. Lalitha and P.T. Manoharan, *J. Electron Spectrosc. Relat. Phemon.*, 1989, **49**, 61.
43 J.M. Tour, L. Jones, D.L. Pearson, J.J.S. Lamba, T.P. Burgin, G.M. Whitesides D.L. Allara, A.N. Parikh and S.V. Atre, *J. Am. Chem. Soc.* 1995, **117**, 9529-9534.
44 M. del Carmen Gimenez-Lopez, M.T. Räisänen, T.W. Chamberlain, U. Weber, M. Lebedeva, G.A. Rance, G.A.D. Briggs, D. Pettifor, V. Burlakov, M. Buck and A.N. Khlobystov*, Langmuir*, 2011, **27**, 10977-10985.
45 J. Heeg, C. Kramer, M. Wolter, S. Michaelis, W. Plieth and W. Fischer, *J. Appl. Surf. Sci.*, 2001, **180**, 36-41.
46 X. Liu, M. Atwater, J. Wang and Q. Huo, *Colloids and Surfaces B: Biointerfaces*, 2007, **58**, 3-7.
47 F. Zhou, C. Jehoulet and A.J. Bard,. *J. Am. Chem. Soc.*, 1992, **114**, 11004-11006.
48 T. Gu, J.K. Whitesell and M. Fox, *J. Org. Chem.*, 2004, **69**, 4075-4080.
49 A.S. Viana, S. Leupold, C. Eberle, T. Shokati, F.P. Montforts, and L.M. Abrantes, *Surf. Sci.*, 2007, **601**, 5062-5068.
50 Q. Xie, E. Perez-Cordero and L. Echegoyen, *J. Am. Chem. Soc.*, 1992, **114**, 3978-3980.
51 Y. Ohsawa and T. Saji, *J. Chem. Soc., Chem. Commun.*, 1992, 781-782.

RSC Advances Accepted Manuscript